Myosin II regulates the shape of three-dimensional intestinal epithelial cysts

Andrei I. Ivanov[1,*,‡], Ann M. Hopkins[2], G. Thomas Brown[1], Kirsten Gerner-Smidt[1], Brian A. Babbin[1], Charles A. Parkos[1] and Asma Nusrat[1]

[1]Epithelial Pathobiology Research Unit, Department of Pathology and Laboratory Medicine, Emory University, Atlanta, GA 30322, USA
[2]Department of Surgery, Royal College of Surgeons in Ireland, Dublin, Ireland

*Present address: Gastroenterology and Hepatology Division, Department of Medicine, University of Rochester School of Medicine, 601 Elmwood Avenue, Box 646, Rochester, NY 14642, USA

‡Author for correspondence (e-mail: Andrei_Ivanov@urmc.rochester.edu)

Accepted 3 March 2008
Journal of Cell Science 121, 1803-1814 Published by The Company of Biologists 2008
doi:10.1242/jcs.015842

Summary

The development of luminal organs begins with the formation of spherical cysts composed of a single layer of epithelial cells. Using a model three-dimensional cell culture, this study examines the role of a cytoskeletal motor, myosin II, in cyst formation. Caco-2 and SK-CO15 intestinal epithelial cells were embedded into Matrigel, and myosin II was inhibited by blebbistatin or siRNA-mediated knockdown. Whereas control cells formed spherical cysts with a smooth surface, inhibition of myosin II induced the outgrowth of F-actin-rich surface protrusions. The development of these protrusions was abrogated after inhibition of F-actin polymerization or of phospholipase C (PLC) activity, as well as after overexpression of a dominant-negative ADF/cofilin. Surface protrusions were enriched in microtubules and their formation was prevented by microtubule depolymerization. Myosin II inhibition caused a loss of peripheral F-actin bundles and a submembranous extension of cortical microtubules. Our findings suggest that inhibition of myosin II eliminates the cortical F-actin barrier, allowing microtubules to reach and activate PLC at the plasma membrane. PLC-dependent stimulation of ADF/cofilin creates actin-filament barbed ends and promotes the outgrowth of F-actin-rich protrusions. We conclude that myosin II regulates the spherical shape of epithelial cysts by controlling actin polymerization at the cyst surface.

Supplementary material available online at
http://jcs.biologists.org/cgi/content/full/121/11/1803/DC1

Key words: Actin polymerization, phospholipase C, ADF/cofilin, Microtubules, Protrusions, Morphogenesis, Tubulogenesis, Matrigel

Introduction

Reorganization of epithelial sheets plays a crucial role in the formation of various luminal organs in metazoans (Lubarsky and Krasnow, 2003; Schock and Perrimon, 2002). Epithelial morphogenesis is a highly complex process involving cell division, migration, cell-cell and cell–extracellular-matrix adhesions, cell shape changes, and apoptosis (O'Brien et al., 2002; Schock and Perrimon, 2002). This process can be modeled in vitro by embedding epithelial cells into three-dimensional (3D) gels of either individual (collagen) or mixed (Matrigel) extracellular matrix proteins (O'Brien et al., 2002; Schmeichel and Bissell, 2003; Walpita and Hay, 2002). In such 3D matrices, colonies of cultured epithelial cells undergo a multistep reorganization from an amorphous aggregate to a spherical cyst, which can be further transformed into linear or branched tubes by stimulation with growth factors (O'Brien et al., 2002).

The formation of cysts is considered to be a crucial step in epithelial morphogenesis in vitro (Lubarsky and Krasnow, 2003; O'Brien et al., 2002). Such cysts represent hollow spheres comprised of monolayers of epithelial cells and they recapitulate a variety of spherical structures (acini, alveoli, follicles) that are formed by epithelial sheets in vivo. Within a cyst, epithelial cells are connected to each other by typical intercellular junctions and are polarized in such a manner that the apical surface of all cells is oriented towards the lumen of the cyst (Lubarsky and Krasnow, 2003; O'Brien et al., 2002). The general architecture of epithelial cysts, specifically the spherical shape and the apico-basal polarization of cell components, strongly suggests that the actin cytoskeleton is involved in the formation and/or maintenance of normal cyst morphology. Indeed, two lines of evidence demonstrate the role of actin filaments in cyst biogenesis. First, disruption of the actin cytoskeleton by cytochalasin D treatment has been reported to prevent the formation of lumen-bearing cysts of cultured rat intestinal epithelial cells (Olson et al., 1991) and human colon carcinoma cells (Lincz et al., 1997). Second, expression of dominant-negative mutants or siRNA-mediated knockdown of major regulators of F-actin organization, Rac1 and Cdc42, have been shown to invert cell polarity in kidney epithelial cysts (Martin-Belmonte et al., 2007; O'Brien et al., 2001). Despite these reports, the role of the actin cytoskeleton in epithelial cystogenesis, and the mechanisms by which F-actin reorganization influences the formation and maintenance of cyst architecture remain poorly understood.

Organization of intracellular F-actin depends on a large family of myosin motor proteins (Cramer, 1999; Maciver, 1996; O'Connell et al., 2007). By hydrolyzing ATP, myosins generate mechanical force to move and bundle actin microfilaments, thereby regulating the architecture and dynamic reorganization of the actin cytoskeleton (De La Cruz and Ostap, 2004; O'Connell et al., 2007). Conventional myosin II is a major protein that drives muscle contraction and is a crucial regulator of motility, cell shape and cytokinesis in non-muscle cells (Cramer, 1999; Maciver, 1996). Several recent studies have implicated myosin II in the regulation of epithelial morphogenesis. For example, this motor protein was found to be important for the formation of intercellular junctions and the

establishment of apico-basal polarity of epithelial cells growing in two-dimensional (2D) monolayers (Ivanov et al., 2005; Zhang et al., 2005). Furthermore, myosin II was shown to drive reorganization of epithelial layers at early stages of embryogenesis in *Drosophila* and zebrafish (Jacinto et al., 2002; Koppen et al., 2006). Finally, recent studies have implicated Rho-dependent kinase in the development of mammalian lung and kidney (Meyer et al., 2006; Moore et al., 2005; Rogers et al., 2003), thereby suggesting a role of myosin II, which is a major downstream effector of Rho-kinase. However, direct evidence of myosin II involvement and the molecular mechanisms by which this motor protein can drive mammalian epithelial morphogenesis are still lacking. The present study was designed to investigate the role of nonmuscle myosin (NMM)II in the formation of 3D intestinal epithelial cysts using an in vitro model: human intestinal epithelial cells grown in a Matrigel matrix.

Results

To investigate the role of myosin II in epithelial morphogenesis, we first analyzed the localization of myosin II in epithelial cysts. Caco-2 cells were embedded in 3D Matrigel, and 72 hours later were fixed and double-labeled for F-actin and either NMMII heavy chain isoform A or isoform B. These NMMII isoforms have been shown to be important for cell and tissue morphogenesis (Brown and Bridgman, 2004; Conti et al., 2004), and to be abundantly expressed in human colonic epithelial cells (Ivanov et al., 2007). As shown in Fig. 1, Matrigel-embedded Caco-2 cells formed spherical cysts with well-developed central lumens. Both NMMIIA and NMMIIB were especially enriched in F-actin bundles that line the basal surface of the cyst (arrows). To gain insight into the functional role of myosin II, we inhibited its activity using S(–)-blebbistatin (Straight et al., 2003) or Y-27632 (Hirose et al., 1998) and examined the effects of this inhibition on the formation of 3D cysts. Blebbistatin and Y-27632 are known to affect NMMII via different mechanisms, with the former blocking the ATPase activity of myosin heavy chain (Kovacs et al., 2004; Straight et al., 2003) and the latter preventing activatory phosphorylation of myosin light chain (Hirose et al., 1998). Initially, S(–)-blebbistatin (100 μM), Y-27632 (20 μM) or vehicle were added at the time of embedding of Caco-2 cells into 3D Matrigel and, 72 hours later, cyst morphology was visualized by labeling for F-actin. Whereas vehicle-treated cells formed cysts with smooth surfaces and central lumens (Fig. 2A), cysts developing in the presence of myosin II inhibitors displayed distinct abnormalities. The most obvious abnormality was the presence of F-actin-rich surface protrusions (Fig. 2A, arrows), which were observed in 78±8% of blebbistatin-treated and 69±7% of Y-27632-treated cysts.

We next investigated whether the formation of peripheral F-actin-rich spikes was associated with dynamic reorganization of 3D cell aggregates during cyst formation, or whether these spikes could also originate from fully differentiated epithelial cells. Preformed Caco-2 epithelial cysts cultured for 72 hours in 3D Matrigel were incubated for an additional 12 hours in the presence of either 100 μM blebbistatin or vehicle. In preformed cysts, inhibition of myosin

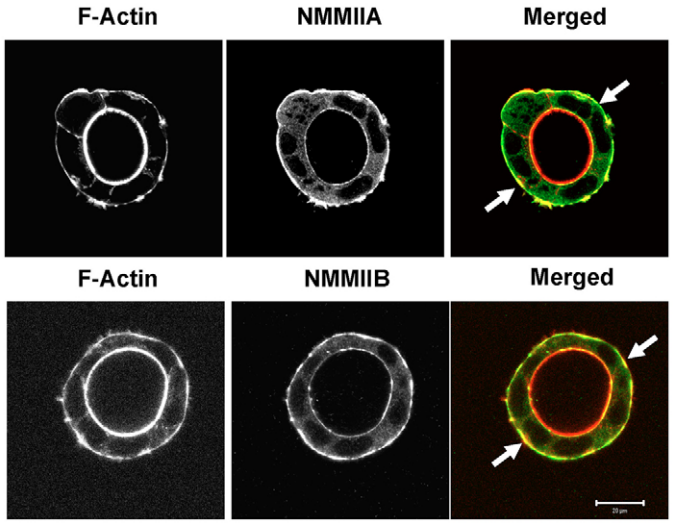

Fig. 1. Myosin II is enriched at the surface of 3D epithelial cysts. Caco-2 cells were embedded in Matrigel for 72 hours, fixed, and fluorescently double-labeled for F-actin (red) and either NMMIIA or NMMIIB (green). Cross-sections of Caco-2 cysts show that significant pools of NMMIIA and NMMIIB accumulate within F-actin bundles at the cyst surface (arrows). Scale bar: 20 μm.

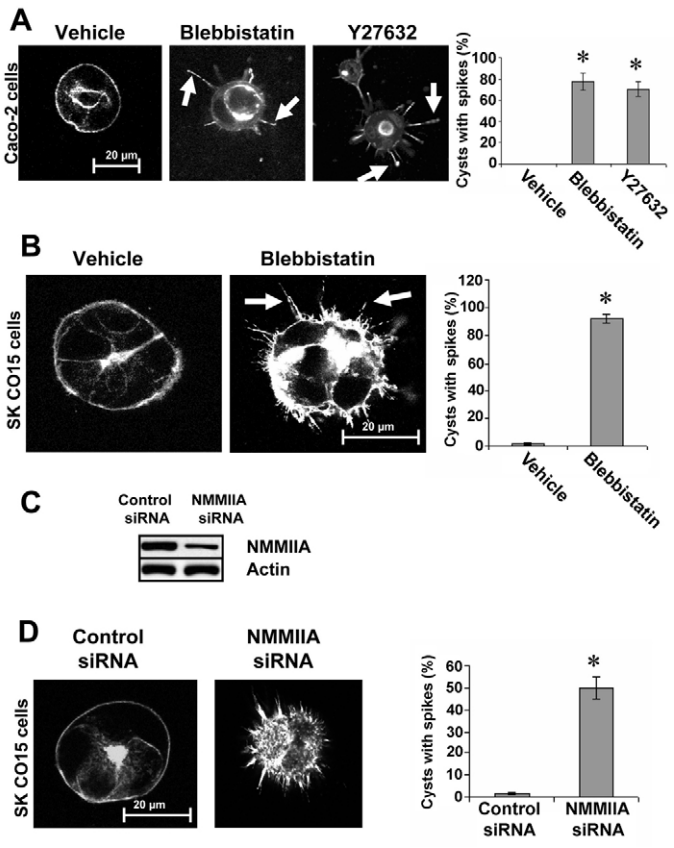

Fig. 2. Inhibition of myosin II causes the formation of F-actin-rich protrusions at the surface of epithelial cysts. (A,B) Caco-2 (A) or SK-CO15 (B) cells were embedded for 72 hours into 3D Matrigel in the presence of either vehicle or the myosin II inhibitors blebbistatin (100 μM) or Y27632 (20 μM) and analyzed for cyst morphology by fluorescent labeling for F-actin. Vehicle-treated Caco-2 and SK-CO15 cells formed spherical cysts with smooth surfaces, whereas cysts grown in the presence of myosin II inhibitors developed radiating F-actin protrusions (arrows). (C,D) SK-CO15 cells were transfected with either control or NMMIIA-specific siRNA and, 72 hours later, were analyzed for NMMIIA expression (C) and morphology of 3D cysts (D). NMMIIA knockdown caused a significant decrease in the level of NMMIIA and induced the formation of numerous F-actin-rich surface spikes. *P<0.05.

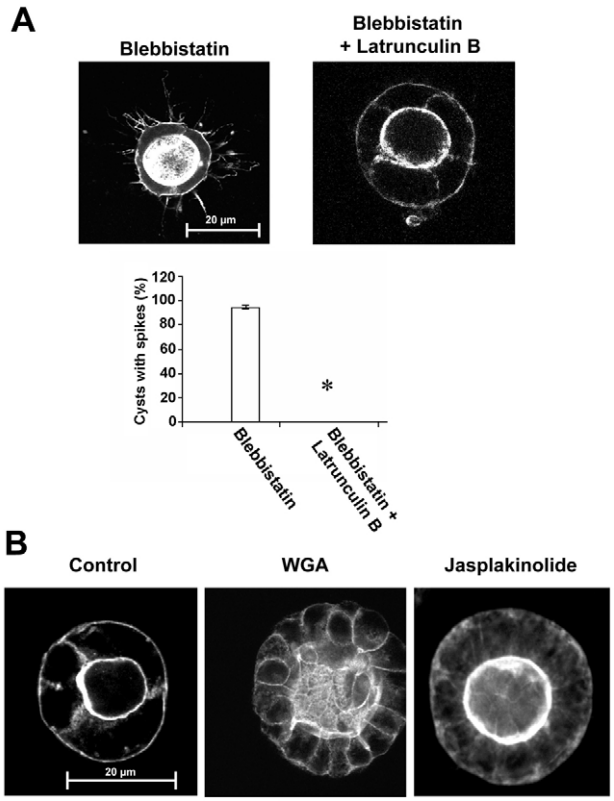

Fig. 3. Formation of peripheral protrusions is mediated by actin polymerization and is not caused by stabilization of cortical F-actin. (A) Preformed Caco-2 cysts were treated for 12 hours with either blebbistatin alone (100 μM) or with a combination of blebbistatin and latrunculin B (1 μM) to inhibit actin polymerization. Inhibition of actin polymerization prevented the formation of peripheral protrusions in blebbistatin-treated Caco-2 cysts (**P*<0.001). (B) Preformed Caco-2 cysts were treated for 12 hours with either vehicle, a cortical flow inhibitor (WGA; 500 μg/ml) or an F-actin-stabilizing drug (jasplakinolide; 0.5 μM). The formation of protrusions on the cyst surface was not induced by any treatment.

II triggered the formation of peripheral protrusions (Fig. 3A) that were undistinguishable from those caused by addition of blebbistatin at the onset of cystogenesis (Fig. 2A). This suggests that the formation of surface spikes reflects changes in the shape of stationary epithelial cells. Given these findings, in subsequent experiments surface spikes were induced by 12 hours of treatment of preformed cysts with blebbistatin.

To ensure that myosin-II-dependent formation of peripheral protrusions does not represent a peculiarity of the Caco-2 cell line, effects of NMMII inhibition were investigated in another human colonic epithelial cell line, SK-CO15 (Ivanov et al., 2006; Le Bivic et al., 1989). Similarly to Caco-2 cells, SK-CO15 cells grow as spherical cysts in 3D Matrigel (Fig. 2B). Furthermore, blebbistatin treatment induced the formation of peripheral protrusions in 93±3% of SK-CO15 cysts, which was significantly higher than the 2.0±0.6% of protrusive cysts found in a vehicle-treated group. To verify that the development of surface protrusions following blebbistatin treatment is not caused by unrelated side effects of this myosin II inhibitor, we examined the effects of siRNA-mediated downregulation of NMMIIA, which was previously shown to alter the shape of individual epithelial cells grown on a 2D surface (Ivanov et al., 2007). SK-CO15 cells transfected with NMMIIA-specific or control siRNAs were embedded into 3D Matrigel, and cyst morphology was analyzed by F-actin labeling and confocal microscopy. As shown in Fig. 2C, transfection with NMMIIA-specific siRNA caused significant (~70%) downregulation of myosin IIA expression in SK-CO15 cells. Consistent with the inhibitor studies, this knockdown induced the formation of peripheral protrusions in 50±5% of SK-CO15 cysts, which was significantly higher than the 1.7±0.6% of protrusive cysts observed in the control siRNA-transfected group (Fig. 2D). Overall, this pharmacological and siRNA-knockdown data suggest that the formation of surface protrusions in 3D intestinal epithelial cysts is a common and direct consequence of myosin II inhibition.

A reasonable hypothesis for these findings is that outgrowth of peripheral F-actin-rich protrusions in stationary epithelial cells is driven by actin polymerization. To test this possibility, we used a pharmacological inhibitor of actin polymerization, latrunculin B. Latrunculins bind to monomeric actin and prevent its incorporation into actin filaments, thus causing depolymerization of dynamic, constantly turning-over filaments (Morton et al., 2000). As shown in Fig. 3A, latrunculin B (1 μM) dramatically decreased the number of spike-bearing Caco-2 cysts from 95±2% in the blebbistatin-only group to 0% in groups treated with the combination of blebbistatin and the F-actin-depolymerizing drug. This finding indicates a key role for actin polymerization in the formation of blebbistatin-induced surface protrusions.

Myosin II is known to promote cortical F-actin dynamics by mechanisms that involve either submembrane flux of actin filaments, known as ‘cortical flow’ (Mandato et al., 2000), or actin-filament severing and/or depolymerization (Guha et al., 2005; Medeiros et al., 2006). Because inhibition of myosin II is likely to result in decreased dynamics of cortical F-actin, we next investigated whether such F-actin stabilization could recapitulate the formation of surface protrusions in epithelial cysts. The dynamics of cortical actin was decreased by either inhibiting cortical flow with tetravalent lectins, such as wheat germ agglutinin [WGA (Canman and Bement, 1997; Rosenblatt et al., 2004)] or by suppressing depolymerization of actin filaments with a cell-permeable drug, jasplakinolide (Bubb et al., 1994). Incubation of Caco-2 cysts for 12 hours with either WGA (500 μg/ml) or jasplakinolide (0.5 μM) did not induce peripheral spikes (Fig. 3B). These results indicate that inhibition of myosin II triggers the formation of surface protrusions by activating signaling pathways to promote actin polymerization and not by decreasing the dynamics of cortical F-actin.

Members of the Rho family of small GTPases, such as Rac1 and Cdc42, are considered as crucial activators of actin polymerization, which drives cell motility and a variety of other cellular processes (Millard et al., 2004; Takenawa and Suetsugu, 2007). We therefore investigated whether Rac1 and Cdc42 play a role in the formation of F-actin-rich protrusions in blebbistatin-treated cysts. For these experiments, we used approaches that included pharmacological inhibitors, expression of dominant-negative mutants and GTPase-activation assays. As shown in Fig. 4A, pharmacological inhibition of Rac with NSC 23766 (100 μM) (Gao et al., 2004) or of Cdc42 with secramine A (20 μM) (Pelish et al., 2006) failed to prevent the formation of blebbistatin-induced surface protrusions in Caco-2 cysts. It is noteworthy that the same concentrations of NSC 23766 and secramine A significantly inhibited motility of Caco-2 cells in a wound-closure model (data not shown), thus confirming the activity of these compounds. Our pharmacological inhibition studies were complemented with the use of Rac1 and Cdc42 dominant-negative mutant constructs expressed in the adenoviral vector. Due

to difficulties in obtaining sufficient numbers of 3D Caco-2 cysts after infection with dominant-negative Rac1 or Cdc42 adenoviruses, this experiment was performed with cells cultured on Matrigel-coated coverslips. Caco-2 cells plated at low density on Matrigel-coated coverslips did not extensively spread but formed compact spheroid colonies (supplementary material Fig. S1). Analogous to the effects observed on 3D cysts, blebbistatin treatment of 2D Caco-2 colonies induced the formation of multiple peripheral protrusions (Fig. 4B). However, cells infected with dominant-negative Rac1- and Cdc42-bearing adenoviruses developed peripheral protrusions upon blebbistatin treatment similarly to cells infected with control EGFP-containing adenovirus (Fig. 4B, arrows). Lastly, we investigated whether blebbistatin activates Rac1 and Cdc42. Caco-2 colonies growing on 2D Matrigel were treated for 12 hours with either blebbistatin or vehicle, and the levels of activated Rac1 and Cdc42 in cell lysates was determined using the PAK1-GST binding assay. As shown in Fig. 4C, blebbistatin treatment did not increase the levels of active Rac1 and Cdc42.

Because Cdc42 and Rac1 promote actin polymerization by activating their down-stream effectors – a neuronal Wiskott-Aldrich syndrome protein (N-WASP) and members of the WASP family verprolin-homologous (WAVE) proteins, respectively – we next investigated whether N-WASP and WAVE1 mediate the formation of peripheral protrusions in myosin-II-inhibited epithelial cysts. We performed siRNA-mediated knockdown of N-WASP and WAVE1 in SK-CO15 cells and analyzed its effect on spike formation. We observed that neither protein knockdown prevented the development of peripheral protrusions in blebbistatin-treated cysts (data not shown). Together, these data suggest that Rac1-WAVE1-mediated and Cdc42–N-WASP-mediated signaling are not involved in the formation of surface spikes in intestinal epithelial cysts induced by myosin II inhibition.

Blebbistatin-induced protrusions on epithelial cysts appeared to be morphologically similar to F-actin-rich neurites observed in stimulated neuronal and neuroendocrine cells. Neurite outgrowth was shown to be dependent on actin polymerization and its upstream signaling events have been extensively characterized (Govek et al., 2005; Sarmiere and Bamburg, 2004; Scott and Luo, 2001). Therefore, to determine the signaling pathway(s) that contribute to the formation of blebbistatin-induced spikes, we analyzed the role of signaling molecules implicated in neurite outgrowth (Gu et al., 2005; Hall et al., 1996; Motegi et al., 2004; Tornieri et al., 2006; Xie et al., 2006). Comprehensive pharmacological screens did not show any effect of inhibitors of tyrosine kinases (genistein, 50 μM; herbimycin A, 2 μM; PP2, 10 μM), mitogen-activated protein kinases (PD 98059, 10 μM; U0126, 5 μM; ERK II inhibitor, 20 μM; SP 600125, 20 μM) or phosphatidylinositol-3 kinase (LY 294002; 20 μM) on the genesis of spikes in blebbistatin-treated Caco-2 cysts (data not shown). However, inhibition of phospholipase C (PLC) with either 1-O-Octadecyl-2-O-methyl-sn-glycero-3-phosphorylcholine (ET-18-OCH_3, 10 μM) (Powis et al., 1992) or U-73122 (1 μM) (Bleasdale et al., 1990) dramatically attenuated the development of peripheral protrusions. As shown in Fig. 5, pharmacological inhibition of PLC significantly decreased the number of spike-bearing cysts from 93±3% in the blebbistatin-only group to 1±1% and 12±1% in cells exposed to ET-18-OCH_3 or U-73122, respectively. Importantly, U-73122 also inhibited development of peripheral protrusions induced by siRNA-mediated depletion of NMMIIA

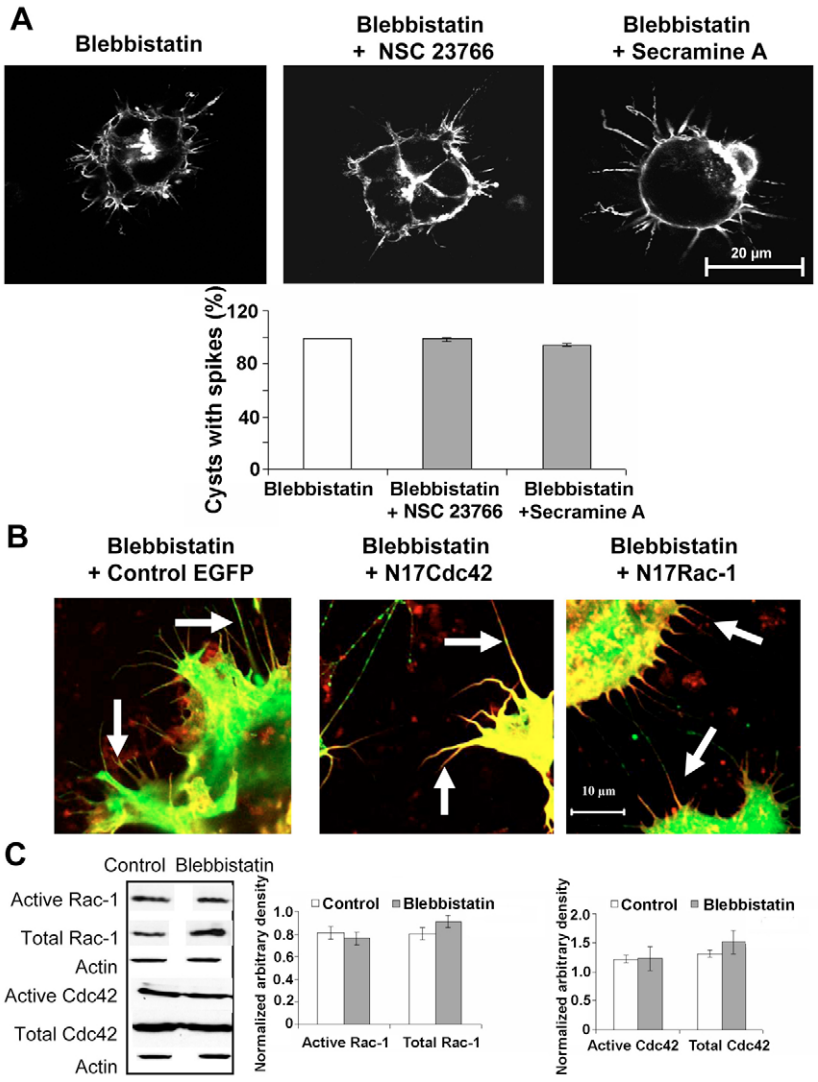

Fig. 4. Activity of Rac1 and Cdc42 is not required for the formation of blebbistatin-induced protrusions. (A) Caco-2 cysts were treated for 12 hours with either blebbistatin alone or in a combination with the Rac inhibitor NSC 23766 (100 μM) or the Cdc42 inhibitor secramine A (20 μM). Pharmacological inhibition of Rac and Cdc42 did not prevent the development of blebbistatin-induced spikes. (B) Caco-2 cells growing on Matrigel-coated coverslips were infected with adenoviruses bearing either control EGFP, or EGFP-tagged dominant-negative N17Rac1 or N17Cdc42 and treated for 12 hours with blebbistatin (100 μM). Cells infected either with control virus or with dominant-negative Rac1 or Cdc42 mutants developed peripheral protrusions upon inhibition of myosin II (arrows). (C) Caco-2 cells were treated for 12 hours with either blebbistatin (100 μM) or vehicle, and activation statuses of Rac1 and Cdc42 were determined in cell lysates using pull-down assays. No increase in the levels of activated Rac1 or Cdc42 were observed in blebbistatin-treated cells.

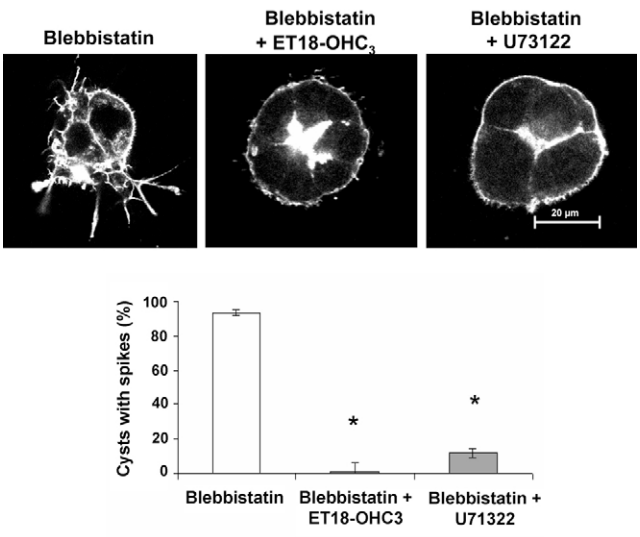

Fig. 5. PLC activity is required for the formation of peripheral protrusions in epithelial cysts. Caco-2 cysts were treated for 12 hours with either blebbistatin alone or in combination with the PLC inhibitors ET-18-OCH_3 (10 μM) or U-73122 (1 μM). Both pharmacological inhibitors of PLC significantly attenuated the formation of blebbistatin-induced spikes (*P<0.001).

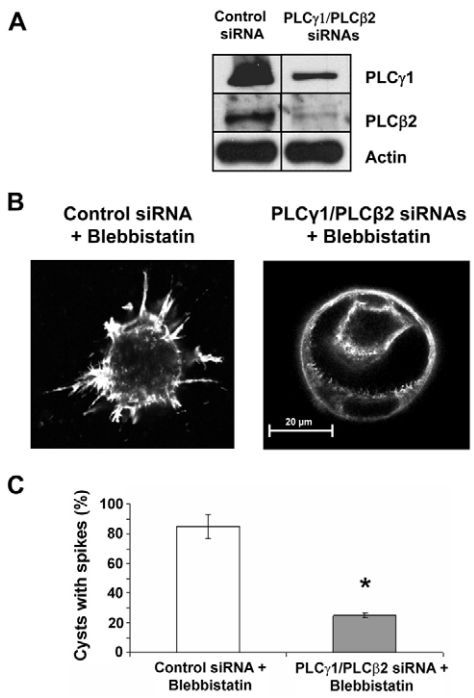

Fig. 6. PLCγ1 and PLCβ2 isoforms mediate the formation of peripheral protrusions in epithelial cysts. SK-CO15 cells were transfected with either control siRNA or a combination of PLCγ1- and PLCβ2-specific siRNAs, embedded into 3D Matrigel and, 72 hours later, were treated with blebbistatin. Dual PLCγ1/PLCβ2 knockdown caused a dramatic decrease in the level of both PLC isoforms (A) and significantly attenuated the formation of F-actin-rich spikes on the cyst surface (B,C) (*P<0.01).

in SK-CO15 cysts (supplementary material Fig. S2). ET-18-OCH_3 and U-73122 are general PLC inhibitors, blocking the activity of several isoforms of this enzyme. However, the PLCγ1 and PLCβ2 isoforms are likely to be important for the spike formation because of their involvement in the F-actin-remodeling and F-actin-dependent processes (Brugnoli et al., 2007; Lian et al., 2005; Mouneimne et al., 2004; Yin and Janmey, 2003). To test this hypothesis, we performed a dual siRNA-mediated knockdown of PLCγ1 and PLCβ2 in SK-CO15 cells. Downregulation of both PLC isoforms (Fig. 6A) did not alter the morphology of control SK-CO15 cysts (data not shown), but significantly decreased the number of spike-bearing cysts after blebbistatin treatment, from 84±3% in the control siRNA-treated group to 25±5% in the PLC-isoforms-depleted group (Fig. 6B,C). Interestingly, individual knockdown of either PLCγ1 or PLCβ2 did not affect spike formation (data not shown), which is likely to reflect a functional redundancy of different PLC isoforms.

We also investigated whether blebbistatin influences the intracellular distribution of PLCγ1, which is important for regulating the local activity of this enzyme on cellular membranes. Immunofluorescence labeling and confocal microscopy revealed the accumulation of PLCγ1 as well as active Ser1248/1249-phosphorylated PLCγ1 (Dittmar et al., 2002; Kim et al., 1991) in the surface protrusions of blebbistatin-treated 3D cysts (Fig. 7A). However, blebbistatin treatment did not affect expression levels of two active forms of PLCγ1 phosphorylated at Tyr783 and Ser1248/1249 in Caco-2 cells (data not shown). These results suggest that myosin II does not modulate phosphorylation-dependent activation of this enzyme. Furthermore, biochemical fractionation of Caco-2 cells detected a significant increase in the amount of membrane-bound PLCγ1 after inhibition of myosin II (Fig. 7B); this might represent an alternative mechanism of PLC activation. Overall, these results highlight a crucial role of PLC activity in the development of F-actin-rich peripheral protrusions induced by myosin II inhibition in intestinal epithelial cysts.

A mechanistic link between PLC activity and reorganizations of the F-actin cytoskeleton is likely to involve PLC-dependent activation of actin-depolymerizing factor (ADF)/cofilin proteins, which are known for their ability to depolymerize and sever actin filaments (Bamburg, 1999; Ono, 2007). Particularly, ADF/cofilin-mediated severing was shown to increase the amount of free actin-filament barbed ends and thus to promote filament polymerization and growth (Wang et al., 2007). Based on these data, we next investigated whether ADF/cofilin proteins play a role in the formation of blebbistatin-induced spikes. Caco-2 cells were embedded for 72 hours into 3D Matrigel in the presence of adenoviruses containing either an EGFP-tagged constitutively inactive S3E cofilin mutant (Suurna et al., 2006) or control EGFP and, 72 hours later, were treated with blebbistatin. Thereafter, cysts were labeled for F-actin and their surface morphology was examined by confocal microscopy. As shown in Fig. 8, overexpression of inactive cofilin significantly decreased the number of spike-bearing cysts from 89±2% in the control EGFP-expressing group to 6±3% in cells expressing the inactive cofilin mutant. Interestingly, overexpression of a constitutively active S3A cofilin mutant induced formation of peripheral processes in control Caco-2 cysts even without myosin II inhibition (Fig. 8C). However, these processes appeared as surface blebs rather than as the linear radial spikes observed in myosin-II-inhibited cysts. Two major conclusions can be made from this observation. One is that ADF/cofilin is involved in the formation of peripheral F-actin-rich spikes by increasing protrusive dynamics of the cyst surface. Another conclusion is that ADF/cofilin activation is not sufficient to mediate spike formation

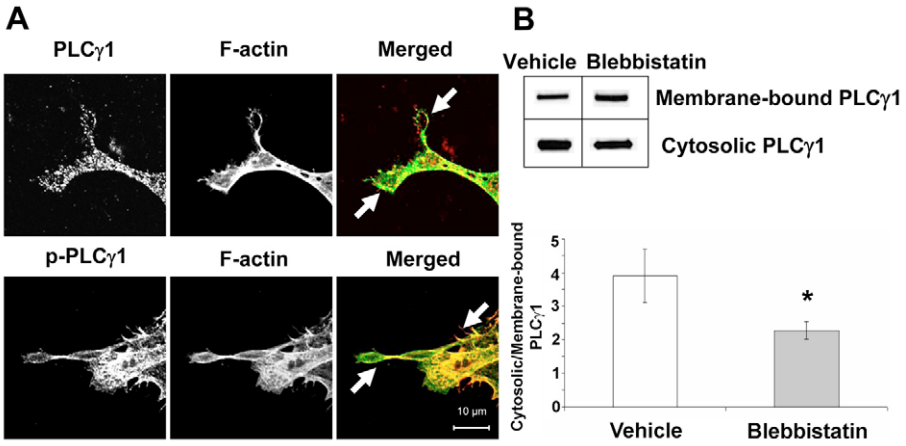

Fig. 7. PLC is localized in surface protrusions and becomes redistributed to a membrane-bound fraction of blebbistatin-treated epithelial cells. (A) Caco-2 cells growing for 72 hours on Matrigel-coated coverslips were treated for 12 hours with blebbistatin (100 μM), fixed, and double-labeled for F-actin (green) and either total or active Ser1248/1249-phosphorylated PLCγ1 (red). Both total and active PLCγ1 localize within blebbistatin-induced F-actin-rich protrusions (arrows). (B) Caco-2 cells were treated with either blebbistatin or vehicle, and the amounts of membrane-bound and cytosolic PLCγ1 were determined by cell fractionation and western blotting. A significant increase in the amount of membrane-bound PLCγ1 was observed after myosin II inhibition (*P<0.05).

in myosin-II-inhibited epithelial cysts and that an additional mechanism is required to transform cofilin-dependent peripheral membrane processes into linear spikes.

To identify this additional mechanism, we investigated the role of microtubules. Our focus on these cytoskeletal structures was based on recent evidence that microtubules regulate the activity and intracellular distribution of PLCγ1 (Chang et al., 2005; Itoh et al., 1996; Ramoni et al., 2001) and that they play a crucial role in neurite outgrowth (Gordon-Weeks, 2004). Microtubules were depolymerized in myosin-II-inhibited Caco-2 cysts by either nocodazole (30 μM) or vinblastin (10 μM) treatment. This microtubule depolymerization dramatically decreased the amount of protrusion-bearing cysts from 86±2% in the blebbistatin-only group to 5±1% and 7±2% in experimental groups exposed to nocodazole and vinblastin. respectively (Fig. 9A). Likewise, vinblastin treatment significantly inhibited the formation of peripheral spikes in SK-CO15 cysts induced by siRNA-mediated downregulation of NMMIIA (supplementary material Fig. S2). Furthermore, immunofluorescence analysis of blebbistatin-treated Caco-2 cysts revealed thick microtubule bundles in the proximal zone of surface protrusions (Fig. 9B, arrows), whereas the distal ends of protrusions were composed predominantly of F-actin. Microtubule reorganization in living cells is regulated by the

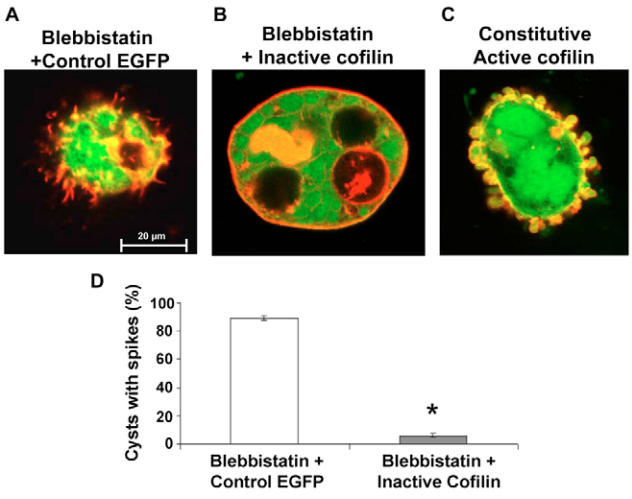

Fig. 8. Cofilin activity is required for the development of surface protrusions in blebbistatin-treated cysts. Caco-2 cells were embedded for 72 hours into 3D Matrigel in the presence of adenoviruses bearing either control EGFP (A) or an EGFP-tagged inactive S3E cofilin mutant (B), followed by 12 hours of treatment with blebbistatin. Inhibition of cofilin activity significantly attenuated the formation of blebbistatin-induced surface protrusions (D) (*P<0.01). (C) Caco-2 cells were grown in 3D Matrigel in the presence of adenoviruses bearing an EGFP-tagged constitutively active S3A cofilin mutant. Overexpression of active cofilin induced the formation of F-actin-rich processes on the cyst surface.

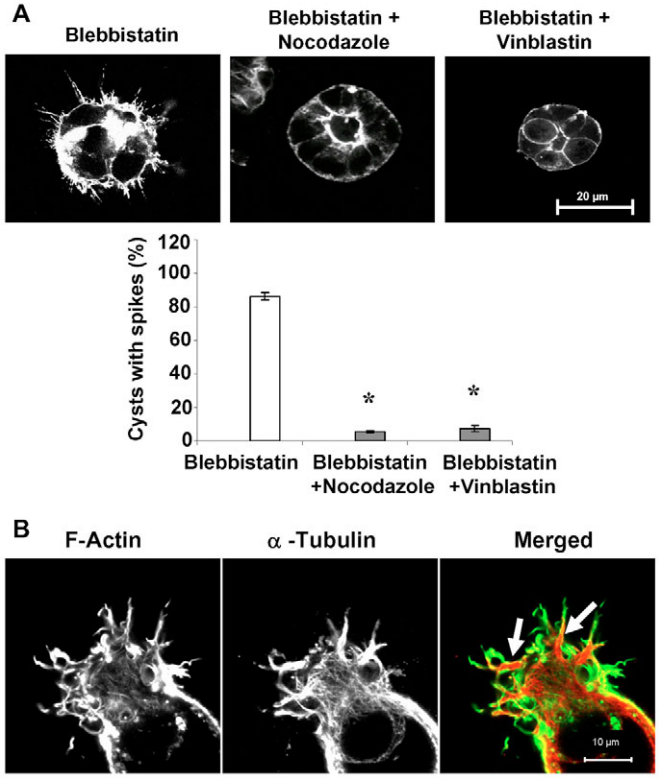

Fig. 9. Microtubules are involved in the formation of blebbistatin-induced protrusions. (A) Preformed Caco-2 cysts were treated for 12 hours with either blebbistatin alone or in combination with the microtubule-depolymerizing drugs nocodazole (30 μM) or vinblastin (10 μM). Microtubule depolymerization prevented the formation of blebbistatin-induced protrusions (*P<0.01). (B) Caco-2 cysts were treated for 12 hours with blebbistatin, fixed, and double-labeled for F-actin (green) and the microtubule marker α-tubulin (red). Microtubules are enriched in the base of blebbistatin-induced spikes (arrows).

dynamic cycle of microtubule extension and shrinkage at their plus ends (Howard and Hyman, 2003). Therefore, we also analyzed whether microtubule plus-end dynamics is important for the formation of F-actin-rich surface protrusions by selectively blocking such dynamics with a low concentration (100 nM) of nocodazole. We observed that this concentration of nocodazole dramatically decreased the number of spike-bearing Caco-2 cysts (from 98% to 7%) caused by blebbistatin treatment (supplementary material Fig. S3).

To gain more insight into the relationships of actin filaments and microtubules after myosin II inhibition, we examined the organization of these cytoskeletal structures in Caco-2 cells cultured on Matrigel-coated coverslips. Double-fluorescence labeling revealed that control cells possessed thick F-actin bundles oriented parallel to the edge of epithelial colonies (Fig. 10A). A dense network of microtubules was localized immediately subjacent to the F-actin bundles (Fig. 10A, arrows). Relatively few parallel-aligned microtubules were detected in the immediate vicinity of the plasma membrane. Inhibition of myosin II was associated with two major changes in the organization of the cortical cytoskeleton. The first was the disappearance of cortical F-actin bundles, which were replaced by a disorganized F-actin network. The second change was the reorientation of microtubules so that they became perpendicular to cell-spreading edges, and their extension into the submembranous compartment (Fig. 10A, arrowheads). We quantified these changes in cortical microtubule distribution by comparing the pixel intensity ratio for the α-tubulin signal at the front versus the back of parallel F-actin bundles in control Caco-2 colonies with the α-tubulin intensity ratio in the distal versus the proximal parts of blebbistatin-induced protrusions. As shown in Fig. 10B, such a tubulin intensity ratio was significantly higher in blebbistatin-induced protrusions, which indicates the enrichment of microtubules in the submembranous space. Furthermore, microtubules in blebbistatin-treated cells appeared to be thicker compared with vehicle-treated controls, suggesting increased stability. This suggestion was supported by Triton X-100 (TX-100) fractionation, which demonstrated a significant increase in the amount of TX-100-insoluble, stable microtubules in blebbistatin-treated Caco-2 cells (supplementary material Fig. S4). Overall, our results show that interplay between microtubules and the F-actin cytoskeleton plays a crucial role in the formation of peripheral protrusions following inhibition of myosin II in intestinal epithelial cells.

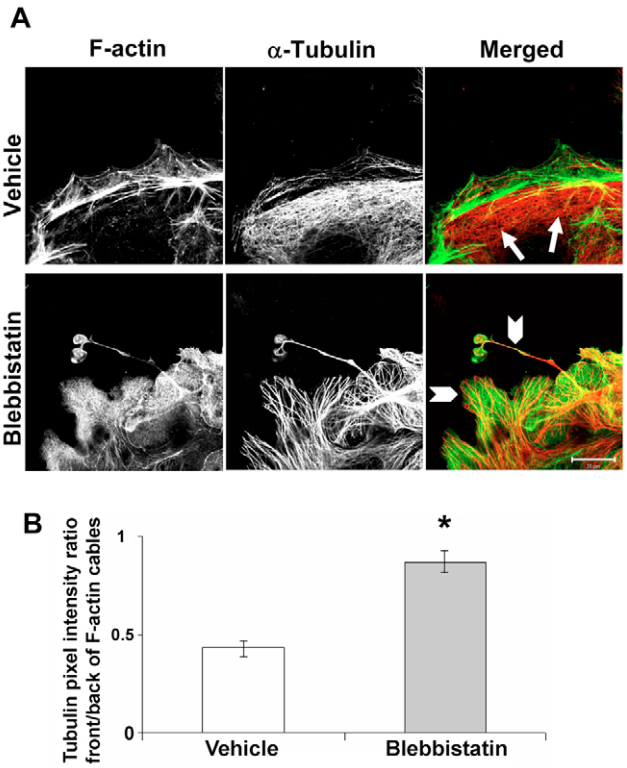

Fig. 10. Blebbistatin treatment triggers the reorientation of cortical microtubules. (A) Caco-2 cells growing on Matrigel-coated coverslips were treated for 12 hours with either blebbistatin (100 μM) or vehicle, fixed, and double-labeled for F-actin (green) and α-tubulin (red). In vehicle-treated cells, cortical microtubules are positioned in parallel to the cell surface behind thick actomyosin bundles (arrows). Blebbistatin treatment induces the disassembly of actomyosin bundles and reorientation of cortical microtubules so that they are perpendicular to the edge of epithelial colonies (arrowheads). Scale bar: 20 μm. (B) Quantification of changes in microtubule distribution. The average pixel intensity ratios were calculated for α-tubulin signal at the front versus the back of F-actin cables in control Caco-2 colonies and in the distal versus proximal parts of peripheral protrusions in blebbistatin-treated colonies. The pixel intensity ratio was significantly higher in blebbistatin-treated cells, thus indicating the accumulation of microtubules in close vicinity to the plasma membrane (*P<0.05).

Discussion

The formation of spherical cysts represents a crucial early step in 3D epithelial morphogenesis. Cysts later transform into tubules that elongate and branch, leading to the development of luminal organs in the body. Studies of model epithelial cysts formed in 3D protein matrices in vitro show that the transformation from a cyst to a tubule involves a directional outgrowth of surface protrusions governed by a gradient of morphogenic factors or other extrinsic cues (O'Brien et al., 2002; Rogers et al., 2003). It is therefore likely that outgrowth of these peripheral spikes is temporally and spatially controlled. Conversely, unregulated protrusiveness at a cyst surface might lead to misshaped tubules and thus to abnormal organogenesis.

In this study, we describe a novel mechanism limiting the outgrowth of peripheral protrusions in 3D intestinal epithelial cysts that involves activity of the major F-actin motor, myosin II. Our data demonstrate the enrichment of myosin II in F-actin bundles that line the basal surface of cysts (Fig. 1). Moreover, pharmacological inhibition or expressional downregulation of myosin II induced the formation of radiating F-actin-rich protrusions on the cyst surface (Fig. 2). This effect of myosin II inhibition has not been previously reported for 3D epithelial cystogenesis. Although acquisition of a protrusive phenotype upon interfering with the functions of myosin II has been observed in individual epithelial and fibroblastic cells in 2D cultures (Even-Ram et al., 2007; Scaife et al., 2003), the mechanisms underlying the formation of these protrusions and development of spikes in 3D cysts are likely to be different. Protrusions induced by inhibition of myosin IIA in individual fibroblasts can occur secondary to attenuated retraction of the cell rear in motile cells (Even-Ram et al., 2007). This retraction mechanism is not plausible in stationary epithelial cells within 3D cysts, in which the formation of peripheral protrusions depends on actin polymerization (Fig. 3A). Interestingly, our pharmacological inhibition analysis indicated that outgrowth of peripheral protrusions in epithelial cysts cannot be explained by simple stabilization of cortical F-actin caused by inhibition of either myosin-II-dependent cortical flow or depolymerization of actin

filaments (Fig. 3B). These findings raise the possibility that inhibition of myosin II activates intracellular signaling events that promote directional actin polymerization at the cyst surface.

Rho GTPases such as Rac1 and Cdc42 represent obvious candidate signaling molecules that could regulate the generation of F-actin-rich epithelial spikes. Indeed, these spikes morphologically resemble filopodia, which are formed at the leading edge of migrating cells or neurite extensions in growing neurons. Filopodial formation is known to be Cdc42-dependent (Nobes and Hall, 1995), and both Cdc42 and Rac1 have been shown to be positive regulators of neurite outgrowth (Govek et al., 2005). Furthermore, a recent study revealed the activation of Rac1 in fibroblasts after inhibition of myosin II activity with blebbistatin or expressional downregulation of NMMIIA (Even-Ram et al., 2007). Surprisingly, our experimental data argue against the roles of Rac1 and Cdc42 in the formation of cell surface protrusions following inhibition of myosin II with blebbistatin. Neither pharmacological inhibitors of these small GTPases nor expression of their dominant-negative mutants abrogated blebbistatin-induced protrusions in 3D Caco-2 cysts or in their corresponding 2D colonies (Fig. 4A,B). Furthermore, blebbistatin treatment failed to increase levels of activated Rac1 and Cdc42 in Caco-2 cells (Fig. 4C). These findings are consistent with our observation that the formation of blebbistatin-induced spikes in SK-CO15 cells does not depend on the activity of N-WASP and WAVE1 (data not shown), which are downstream effectors of Cdc42 and Rac1 signaling (Millard et al., 2004; Takenawa and Suetsugu, 2007). These data, together with the study in fibroblasts, indicate that the formation of peripheral protrusions triggered by myosin II inhibition can be mediated via multiple cell-specific mechanisms.

In a search for alternative intracellular signals that could contribute to the formation of peripheral F-actin-rich protrusions following myosin II inhibition in intestinal epithelial cysts, we demonstrated a role of PLC. Supporting evidence includes attenuation of spike formation by pharmacological PLC inhibitors (Fig. 5; supplementary material Fig. S2) and by dual siRNA-mediated knockdown of PLCγ1/β2 isoforms (Fig. 6), localization of total and active PLCγ1 in blebbistatin-induced cell surface protrusions (Fig. 7A), and membrane translocation of PLCγ1 upon myosin II inhibition (Fig. 7B). Our data are consistent with the known morphogenic roles of PLC, which has been previously implicated in neurite outgrowth (Hall et al., 1996; Xie et al., 2006) and in growth-factor-induced formation of epithelial (Gual et al., 2000) and endothelial (Meyer et al., 2003) tubules.

How can PLC signaling be involved in the development of F-actin-rich protrusions? PLC is known to hydrolyze phosphatidylinositol (4,5)-bisphosphate [PtdIns(4,5)P_2], leading to the generation of inositol (1,4,5)-trisphosphate [Ins(1,4,5)P_3] and diacylglycerol (Lee and Rhee, 1995). All of these lipid mediators are potent regulators of F-actin dynamics. For example, PtdIns(4,5)P_2 directly interacts with and modulates the activity of a number of actin-binding proteins, including ADF/cofilin, profilin, gelsolin, villin and α-actinin (Yin and Janmey, 2003). Ins(1,4,5)P_3 triggers Ca^{2+} release from intracellular stores and thus can activate Ca^{2+}-dependent regulators of the actin cytoskeleton, whereas diacylglycerol affects actin dynamics by activating protein kinase C (Larsson, 2006). Our results suggest that one of these downstream effectors of PLC mediates the outgrowth of peripheral F-actin-rich protrusions in myosin-II-inhibited epithelial cysts. Indeed, we demonstrated that the formation of surface spikes can be inhibited by overexpression of the inactive cofilin mutant (Fig. 8), whereas expression of the constitutively active cofilin mutant was sufficient to stimulate formation of F-actin-rich processes at the cyst surface even without inhibition of myosin II (Fig. 8C). ADF and cofilin are known F-actin-severing proteins (Bamburg, 1999; Ono, 2007), and severing of actin filaments was shown to create free barbed ends, thus promoting filamentous outgrowth (Cramer, 1999; Wang et al., 2007). Our results implicating PLC and cofilin in the development of F-actin-rich surface protrusions are in agreement with previous findings that PLC positively regulates the severing of actin filaments by stimulating ADF/cofilin activity (Lee and Rhee, 1995). Such PLC-dependent activation of ADF/cofilin appears to be a crucial driving force for actin polymerization at the leading edge of migrating epithelial and fibroblastic cells (Mouneimne et al., 2006; Mouneimne et al., 2004; Wang et al., 2007). Furthermore, overexpression of ADF (Meberg and Bamburg, 2000) was shown to enhance the outgrowth of peripheral protrusions in primary neurons and neuroendocrine cells, whereas siRNA-mediated knockdown of cofilin or ADF dramatically abrogated neurite extension (Endo et al., 2007).

The mechanism whereby inhibition of myosin II activates PLC signaling remains to be elucidated. Although the major mechanism of PLCγ1 activation involves its tyrosine and serine phosphorylation (Bourguignon et al., 2004; Dittmar et al., 2002; Kim et al., 1991), such activation modes are unlikely to be responsible for the formation of epithelial protrusions. Indeed, the level of PLCγ1 that was phosphorylated at Tyr783 and Ser1248/1249 was not increased in blebbistatin-treated cells, nor did inhibition of tyrosine kinases prevent spike formation (data not shown). Our data suggest an alternative mechanism regulating PLC activity in blebbistatin-treated cysts; this mechanism might involve translocation of PLCγ1 to the plasma membrane (Fig. 7).

PLC-dependent activation of ADF/cofilin alone is unlikely to be sufficient in inducing surface protrusions in epithelial cysts. In particular, cofilin activation does not result in directional outgrowth of radial F-actin-rich protrusions but rather induces the formation of F-actin blebs at a cyst surface (Fig. 8C). Directionality of spike outgrowth could be determined by other cytoskeletal structures, and our data suggest a crucial role for microtubules in this process. Indeed, the development of peripheral protrusions caused by either pharmacological or siRNA-mediated inhibition of myosin II was dramatically attenuated after depolymerization of microtubules (Fig. 9A; supplementary material Figs S2 and S3). Furthermore, these spikes contained a core of thick microtubule bundles with F-actin concentrated on their tips (Fig. 9B). The involvement of microtubules appears to be a common mechanism for the development of peripheral protrusions observed in growth cones of migrating neurons (Gordon-Weeks, 2004) as well as in fibroblasts challenged by growth factors and myosin II inhibitors (Rhee et al., 2007; Scaife et al., 2003).

The observed interplay between F-actin and microtubules during the generation of epithelial spikes raises two major questions: how might myosin II inhibition affect the structure and/or dynamics of cortical microtubules, and how might changes in microtubule organization trigger polymerization of F-actin? Our double-fluorescence labeling analysis revealed that blebbistatin treatment induces the disassembly of peripheral F-actin bundles, which leads to the reorientation of cortical microtubules and to their extension into the submembranous compartment (Fig. 10). Interestingly, a similar accumulation of microtubules in close proximity to the plasma membrane has been previously reported in neuronal growth cones (Zhou et al., 2002) and fibroblast lamellipodia (Even-Ram

et al., 2007) after disassembly of F-actin bundles by exposure to cytochalasin D and blebbistatin, respectively. In addition to the reorientation of cortical microtubules, blebbistatin also causes a noticeable bundling (Fig. 10A) and increase in stability of microtubules in Caco-2 cells (supplementary material Fig. S4). These results are consistent with recent live-cell imaging analyses demonstrating a significant decrease in the turnover (extension and shrinkage) of cortical microtubules in fibroblasts and epithelial cells after pharmacological inhibition of either myosin II itself (Even-Ram et al., 2007) or its activator, myosin light chain kinase (Yvon et al., 2001). Taken together, these data suggest that loss of cortical actin filaments following myosin II inhibition dramatically affects the spatial distribution of microtubules, leading to their outgrowth to the submembranous compartment and initiation of peripheral protrusions.

Some steps in the signaling cascade controlling microtubule-dependent actin polymerization remain poorly understood. Two different mechanisms underlying microtubule-dependent growth of actin filaments have been described. The first involves activation of actin-polymerizing proteins, formins, at the dynamic microtubule tip (Martin et al., 2005). The second implicates the activation of Rac by growing microtubules (Waterman-Storer et al., 1999). However, the first mechanism has been described in yeast and has not been proved in mammalian cells, whereas the second mechanism cannot explain Rac-independent formation of peripheral protrusions in blebbistatin-treated epithelial cells (Fig. 4). The observed role of PLC in cell surface spike formation might provide yet another mechanism linking cortical microtubules and actin polymerization. Indeed, PLCγ1 is known to physically interact with a major microtubule component, β-tubulin (Chang et al., 2005; Itoh et al., 1996), and such an interaction has been shown to stimulate PLC activity (Chang et al., 2005). In addition, another study observed an interaction of PLCγ1 with the microtubule motors kinesins and suggested microtubule-dependent translocation of cytoplasmic PLCγ1 to the plasma membrane (Ramoni et al., 2001). Similar events can be envisioned in myosin-II-inhibited epithelial cells, in which the reorganization of cortical microtubules might increase the level and/or activity of PLC at the plasma membrane, thereby stimulating actin polymerization on microtubule tips and the formation of surface protrusions.

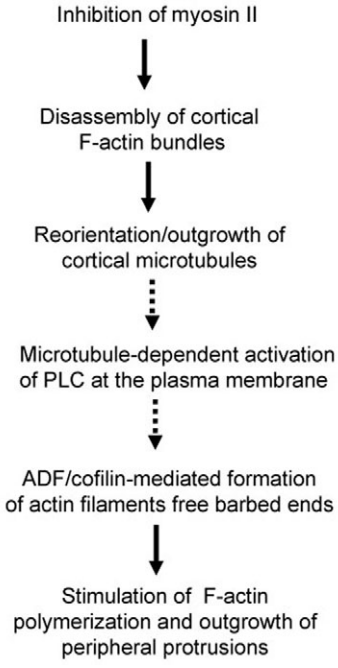

Fig. 11. Hypothetic mechanism for surface protrusion formation in myosin-II-inhibited intestinal epithelial cysts. The diagram depicts key signaling and morphological events involved in the development of peripheral spikes. For simplicity, these events are presented as a single cascade. Tentative and/or unproven connections between different steps in the cascade are marked by broken lines. See explanation in the Discussion.

In conclusion, we propose a hypothetical mechanism that drives the formation of peripheral spikes after inhibition of myosin II in intestinal epithelial cells (Fig. 11). Upon myosin II inhibition, loss of cortical actomyosin bundles leads to the reorientation and/or stabilization of underlying microtubules and their outgrowth into the submembranous compartment. This microtubule outgrowth increases PLC activity at the plasma membrane by either transporting these enzymes from the cytoplasm or by stimulating the activity of resident PLC at the plasma membrane. Activation of PLC stimulates the actin-severing activity of ADF/cofilin, causing a local increase in free actin-filament barbed ends near the interface of microtubule tips and the plasma membrane. This event triggers actin polymerization at microtubule tips leading to the outgrowth of peripheral protrusions. The described mechanism might be important for epithelial morphogenesis in vivo, in which normal activity of myosin II is likely to suppress excessive protrusiveness of the surface of epithelial cysts, thus preventing unregulated alterations in cell shape. By contrast, local inhibition of myosin II by paracrine or cell-bound morphogenic factors might trigger the development of membrane extensions and regulated alterations of cell shape, which are both necessary for initial transformation between the cyst and the tubule as well as later for tubule branching. Further studies are required to validate this role of myosin II in epithelial morphogenesis in vivo.

Materials and Methods

Antibodies and other reagents

The following primary polyclonal (pAb) and monoclonal (mAb) antibodies were used to detect cytoskeletal proteins by immunofluorescence labeling and western blotting: anti-Cdc42, -PLCγ1, -PLCβ2 pAbs (sc-87, sc-426 and sc-206, respectively; Santa Cruz Biotechnology, Santa Cruz, CA); anti-Rac1 mAb (ARC03; Cytoskeleton); anti-phospho-PLCγ1 (Tyr783) pAb (#2821; Cell Signaling Technology, Danver, MA); phospho-PLCγ1 (Ser1248/1249) pAb (#07-511; Upstate, Charlottesville, VA); anti-mammalian nonmuscle myosin IIA and IIB pAbs (PRB-440P and PRB-445P, respectively; Covance, Berkley, CA); anti-α-tubulin mAb (#T6199; Sigma-Aldrich, St Louis, MO). Alexa-Fluor-488-labeled phalloidin and secondary antibodies were obtained from Molecular Probes (Eugene, OR); horseradish-peroxidase-conjugated secondary antibodies were obtained from Jackson ImmunoResearch Laboratories (West Grove, PA).

Rac and/or Cdc42 activation assay kits were purchased from Upstate. Secramine A was provided by Tomas Kirchhausen, Matthew D. Shair, Henry E. Pelish (Harvard Medical School, Boston, MA) and Gerald B. Hammond (University of Louisville, KY) (Xu et al., 2006). NSC23766 was provided by Yi Zheng (Children Hospital Research Foundation, Cincinnati, OH). S(–)-blebbistatin, Y27632, jasplakinolide, wiskostatin, SP 600125, U0126, ERKII inhibitor, PD 98059, LY 294002 and Herbimycin A were obtained from Calbiochem (La Jolla, CA); U23122, vinblastin, nocodazole, genistein and WGA were obtained from Sigma. ET-18-OCH_3 was purchased from Biomol.

3D epithelial cell culture

Caco-2 (American Type Culture Collection, Manassas, VA) and SK-CO15 (gift of Enrique Rodriguez-Boulan, Weill Medical College of Cornell University, NY) human colonic epithelial cell lines were cultured in high glucose Dulbecco's minimal essential medium (DMEM) supplemented with 15 mM HEPES, 40 μg/ml penicillin, 100 μg/ml streptomycin and 10% fetal bovine serum (pH 7.4). Cells were resuspended in DMEM medium and mixed with growth-factor-reduced Matrigel (BD Biosciences, Franklin Lakes, NJ). For each experiment, approximately 10^6 cells were embedded into 200 μl of 30-35% Matrigel. A 3D matrix was allowed to harden in a 96-well

plate at 37°C for 30 minutes, then DMEM medium was added and cysts were allowed to form over 3-4 days at 37°C. Pharmacological inhibitors were added to the medium at concentrations indicated in the Results and figure legends. Stock solutions of water-insoluble inhibitors were prepared in DMSO and diluted in cell culture media immediately before each experiment. The final concentration of DMSO was 0.1% and was included in appropriate controls.

2D cell culture

Caco-2 cells were plated onto 12-mm glass coverslips coated with a thin layer of 30% Matrigel. Cells were allowed to grow for 3-4 days at 37°C before challenging with pharmacological agents or infecting with adenoviruses. Adenoviruses expressing EGFP-tagged dominant-negative mutants N17Rac1 and N17Cdc42, a constitutively inactive S3E mutant of *Xenopus* cofilin as well as control EGFP virus were provided by James Bamburg (University of Colorado, CO) and were produced as described previously (Minamide et al., 2003; Suurna et al., 2006). Cells were incubated in DMEM containing purified viral particles diluted to 5×10^5 plaque-forming units/ml for 2-3 days before treatment with blebbistatin.

Immunofluorescence labeling and confocal microscopy

Caco-2 cells growing on coverslips were fixed with either absolute ethanol or 4% paraformaldehyde and fluorescently labeled as previously described (Ivanov et al., 2005; Ivanov et al., 2006). For visualization of F-actin and myosin II in 3D cultures, Matrigel fragments were fixed for 1 hour in 4% paraformaldehyde, permeabilized for 30 minutes with 0.5% TX-100, blocked overnight with 3% bovine serum albumin at 4°C, incubated for 2 hours at room temperature with primary anti-myosin II antibodies followed by 2 hours of incubation with Alexa-Fluor-488-conjugated phalloidin and secondary antibodies, and mounted with a 1:1:0.01 (v/v/v) PBS/glycerol/*p*-phenylenediamine mixture. Labeled cells were examined using a Zeiss LSM510 Meta laser scanning confocal microscope (Zeiss Microimaging, Thornwood, NY). Fluorescent dyes were imaged sequentially in frame-interlace mode to eliminate fluorescence bleed-over between channels. Images were processed using LSM5 browser software and Adobe Photoshop. For the 3D system, images demonstrate a single confocal section acquired at the center of the cyst. Cysts possessing spikes were counted across at least ten different 40× fields and expressed as a percentage of total cysts. At least 70 cysts were examined per experimental group.

Immunoblotting

Cells were homogenized in a RIPA lysis buffer (20 mM Tris, 50 mM NaCl, 2 mM EDTA, 2 mM EGTA, 1% sodium deoxycholate, 1% TX-100 and 0.1% SDS, pH 7.4) containing proteinase- and phosphatase-inhibitor cocktails (Sigma). Polyacrylamide gel electrophoresis and western blotting were conducted by standard protocols with 10-20 μg protein per lane. Results shown are representative immunoblots of three independent experiments. Protein expression was quantified by densitometric analysis of western blot images on UN-SCAN-IT digitizing software (Silk Scientific, Orem, UT).

Rac and Cdc42 activation assay

Activation status of Rac1 and Cdc42 was determined using commercially available activation assays according to the manufacturer protocols. Briefly, cell lysates were cleared by centrifugation (14,000 ***g*** for 15 minutes) and supernatants were incubated with recombinant PAK1-GST coupled to agarose beads (45 minutes, 4°C with rotation). Beads were washed and resuspended in SDS sample buffer for western blot analysis using anti-Rac1 and anti-Cdc42 antibodies. Whole-cell lysates prepared in the same experiment were also subjected to immunoblotting to show levels of total (active plus inactive) Rac1 and Cdc42.

Membrane preparation

Cells were harvested in relax buffer (100 mM KCl, 3 mM NaCl, 3.5 mM $MgCl_2$, 10 mM HEPES, pH 7.4) containing protease- and phosphatase-inhibitor cocktails, and was nitrogen-cavitated (200 psi, 15 minutes). Nuclei were removed by centrifugation (1000 ***g*** for 10 minutes). Membranes were pelleted by ultracentrifugation of the post-nuclear supernatants at 170,000 ***g*** for 45 minutes. Supernatants (cytosolic fraction) were collected and the pellets were resuspended in an equivalent volume (equivalent to the starting volume of cell lysate) of Hanks balanced salt solution ($HBSS^+$) containing 1% n-octylglucoside by sonication on ice. Equal volumes of the cytosolic and membrane fractions were subjected to immunoblotting analysis as described above.

Microtubule fractionation

Relative amounts of stable and unstable microtubules in control and blebbistatin-treated cells were determined using detergent fractionation of the cells. Caco-2 colonies growing on Matrigel were washed with $HBSS^+$ and were gently rotated for 5 minutes at room temperature with extraction buffer (80 mM Pipes, 1 mM $MgCl_2$, 2 mM EGTA, 0.15% TX-100, pH 6.9) supplemented with proteinase- and phosphatase-inhibitor cocktails (Sigma). The extraction solution was removed, mixed with an equal volume of 2X-SDS sample buffer and boiled. The TX-100-insoluble fraction was collected by scraping pre-extracted, filter-bound cells in two volumes of 1X-SDS sample buffer with subsequent homogenizing and boiling. The amount of α-tubulin in each fraction was determined by electrophoresis and western blotting.

RNA interference

siRNA-mediated knockdown of NMMIIA was carried out using three isoform-specific siRNA duplexes: 5′-GCACAGAGCUGGCCGACAAUU-3′; 5′-GGC-CAAACCUGCCGAAUAAUU-3′ and 5′-GAACAUGGCCCUCAAGAAGUU-3′ (Dharmacon, Lafayette, CO). Downregulation of PLCγ1, PLCβ2, N-WASP and WAVE1 expression was performed using protein-specific siRNA SmartPools (Dharmacon). Cyclophilin B siRNA SmartPool was used as a control. SK-CO15 cells were transfected using the DharmaFect 1 transfection reagent (Dharmacon) in Opti-MEM I medium (Invitrogen), according to the manufacturer's protocol, with a final siRNA concentration of 100 nM. Cells on six-well plates were transfected with siRNA, embedded into Matrigel 12 hours later and allowed to form cysts for an additional 72 hours.

Statistics

Numerical values from three different experiments were pooled and expressed as mean ± s.e.m. throughout. Obtained numbers were compared by a single-tailed Student's *t*-test, with statistical significance assumed at $P<0.05$.

The authors thank Susan Voss, A'Drian Pineda and Moshe Bachar for excellent technical assistance. We are grateful to Enrique Rodriguez-Boulan for the gift of SK-CO15 cells; Tomas Kirchhausen, Matthew D. Shair, Henry E. Pelish and Gerald B. Hammond for providing secramine A; and to James Bamburg and Yi Zheng for providing adenoviral constructs and pharmacological Rac inhibitor. This work was supported by a Career Development Award from the Crohn's and Colitis Foundation of America (to A.I.I.); a CCFA Fellowship Award (to A.M.H.); and by National Institutes of Health grants DK 61379 and DK 72564 (to C.A.P.), DK 55679 and DK 59888 (to A.N.), and a Digestive Diseases minicenter grant DK 064399.

References

Bamburg, J. R. (1999). Proteins of the ADF/cofilin family: essential regulators of actin dynamics. *Annu. Rev. Cell Dev. Biol.* **15**, 185-230.

Bleasdale, J. E., Thakur, N. R., Gremban, R. S., Bundy, G. L., Fitzpatrick, F. A., Smith, R. J. and Bunting, S. (1990). Selective inhibition of receptor-coupled phospholipase C-dependent processes in human platelets and polymorphonuclear neutrophils. *J. Pharmacol. Exp. Ther.* **255**, 756-768.

Bourguignon, L. Y., Singleton, P. A. and Diedrich, F. (2004). Hyaluronan-CD44 interaction with Rac1-dependent protein kinase N-γ promotes phospholipase Cγ1 activation, Ca^{2+} signaling, and cortactin-cytoskeleton function leading to keratinocyte adhesion and differentiation. *J. Biol. Chem.* **279**, 29654-29669.

Brown, M. E. and Bridgman, P. C. (2004). Myosin function in nervous and sensory systems. *J. Neurobiol.* **58**, 118-130.

Brugnoli, F., Bavelloni, A., Benedusi, M., Capitani, S. and Bertagnolo, V. (2007). PLC-β2 activity on actin-associate phosphoinositides promotes migration of differentiating tumor myeloid precursors. *Cell. Signal.* **8**, 1701-1712.

Bubb, M. R., Senderowicz, A. M., Sausville, E. A., Duncan, K. L. and Korn, E. D. (1994). Jasplakinolide, a cytotoxic natural product, induces actin polymerization and competitively inhibits the binding of phalloidin to F-actin. *J. Biol. Chem.* **269**, 14869-14871.

Canman, J. C. and Bement, W. M. (1997). Microtubules suppress actomyosin-based cortical flow in Xenopus oocytes. *J. Cell Sci.* **110**, 1907-1917.

Chang, J. S., Kim, S. K., Kwon, T. K., Bae, S. S., Min, D. S., Lee, Y. H., Kim, S. O., Seo, J. K., Choi, J. H. and Suh, P. G. (2005). Pleckstrin homology domains of phospholipase C-γ1 directly interact with beta-tubulin for activation of phospholipase C-γ1 and reciprocal modulation of beta-tubulin function in microtubule assembly. *J. Biol. Chem.* **280**, 6897-6905.

Conti, M. A., Even-Ram, S., Liu, C., Yamada, K. M. and Adelstein, R. S. (2004). Defects in cell adhesion and the visceral endoderm following ablation of nonmuscle myosin heavy chain II-A in mice. *J. Biol. Chem.* **279**, 41263-41266.

Cramer, L. P. (1999). Organization and polarity of actin filament networks in cells: implications for the mechanism of myosin-based cell motility. *Biochem. Soc. Symp.* **65**, 173-205.

De La Cruz, E. M. and Ostap, E. M. (2004). Relating biochemistry and function in the myosin superfamily. *Curr. Opin. Cell Biol.* **16**, 61-67.

Dittmar, T., Husemann, A., Schewe, Y., Nofer, J. R., Niggemann, B., Zanker, K. S. and Brandt, B. H. (2002). Induction of cancer cell migration by epidermal growth factor is initiated by specific phosphorylation of tyrosine 1248 of c-erbB-2 receptor via EGFR. *FASEB J.* **16**, 1823-1825.

Endo, M., Ohashi, K. and Mizuno, K. (2007). LIM kinase and slingshot are critical for neurite extension. *J. Biol. Chem.* **282**, 13692-13702.

Even-Ram, S., Doyle, A. D., Conti, M. A., Matsumoto, K., Adelstein, R. S. and Yamada, K. M. (2007). Myosin IIA regulates cell motility and actomyosin-microtubule crosstalk. *Nat. Cell Biol.* **9**, 299-309.

Gao, Y., Dickerson, J. B., Guo, F., Zheng, J. and Zheng, Y. (2004). Rational design and characterization of a Rac GTPase-specific small molecule inhibitor. *Proc. Natl. Acad. Sci. USA* **101**, 7618-7623.
Gordon-Weeks, P. R. (2004). Microtubules and growth cone function. *J. Neurobiol.* **58**, 70-83.
Govek, E. E., Newey, S. E. and Van Aelst, L. (2005). The role of the Rho GTPases in neuronal development. *Genes Dev.* **19**, 1-49.
Gu, C., Shim, S., Shin, J., Kim, J., Park, J., Han, K. and Park, S. (2005). The EphA8 receptor induces sustained MAP kinase activation to promote neurite outgrowth in neuronal cells. *Oncogene* **24**, 4243-4256.
Gual, P., Giordano, S., Williams, T. A., Rocchi, S., Van Obberghen, E. and Comoglio, P. M. (2000). Sustained recruitment of phospholipase C-γ to Gαβ1 is required for HGF-induced branching tubulogenesis. *Oncogene* **19**, 1509-1518.
Guha, M., Zhou, M. and Wang, Y. L. (2005). Cortical actin turnover during cytokinesis requires myosin II. *Curr. Biol.* **15**, 732-736.
Hall, H., Williams, E. J., Moore, S. E., Walsh, F. S., Prochiantz, A. and Doherty, P. (1996). Inhibition of FGF-stimulated phosphatidylinositol hydrolysis and neurite outgrowth by a cell-membrane permeable phosphopeptide. *Curr. Biol.* **6**, 580-587.
Hirose, M., Ishizaki, T., Watanabe, N., Uehata, M., Kranenburg, O., Moolenaar, W. H., Matsumura, F., Maekawa, M., Bito, H. and Narumiya, S. (1998). Molecular dissection of the Rho-associated protein kinase (p160ROCK)-regulated neurite remodeling in neuroblastoma N1E-115 cells. *J. Cell Biol.* **141**, 1625-1636.
Howard, J. and Hyman, A. A. (2003). Dynamics and mechanics of the microtubule plus end. *Nature* **422**, 753-758.
Itoh, T., Miura, K., Miki, H. and Takenawa, T. (1996). β-tubulin binds Src homology 2 domains through a region different from the tyrosine-phosphorylated protein-recognizing site. *J. Biol. Chem.* **271**, 27931-27935.
Ivanov, A. I., Hunt, D., Utech, M., Nusrat, A. and Parkos, C. A. (2005). Differential roles for actin polymerization and a myosin II motor in assembly of the epithelial apical junctional complex. *Mol. Biol. Cell* **16**, 2636-2650.
Ivanov, A. I., McCall, I. C., Babbin, B., Samarin, S. N., Nusrat, A. and Parkos, C. A. (2006). Microtubules regulate disassembly of epithelial apical junctions. *BMC Cell Biol.* **7**, 12.
Ivanov, A. I., Bachar, M., Babbin, B. A., Adelstein, R. S., Nusrat, A. and Parkos, C. A. (2007). A unique role for nonmuscle myosin heavy chain IIA in regulation of epithelial apical junctions. *PLoS ONE* **2**, e685.
Jacinto, A., Wood, W., Woolner, S., Hiley, C., Turner, L., Wilson, C., Martinez-Arias, A. and Martin, P. (2002). Dynamic analysis of actin cable function during *Drosophila* dorsal closure. *Curr. Biol.* **12**, 1245-1250.
Kim, H. K., Kim, J. W., Zilberstein, A., Margolis, B., Kim, J. G., Schlessinger, J. and Rhee, S. G. (1991). PDGF stimulation of inositol phospholipid hydrolysis requires PLC-γ1 phosphorylation on tyrosine residues 783 and 1254. *Cell* **65**, 435-441.
Koppen, M., Fernandez, B. G., Carvalho, L., Jacinto, A. and Heisenberg, C. P. (2006). Coordinated cell-shape changes control epithelial movement in zebrafish and *Drosophila*. *Development* **133**, 2671-2681.
Kovacs, M., Toth, J., Hetenyi, C., Malnasi-Csizmadia, A. and Sellers, J. R. (2004). Mechanism of blebbistatin inhibition of myosin II. *J. Biol. Chem.* **279**, 35557-35563.
Larsson, C. (2006). Protein kinase C and the regulation of the actin cytoskeleton. *Cell. Signal.* **18**, 276-284.
Le Bivic, A., Real, F. X. and Rodriguez-Boulan, E. (1989). Vectorial targeting of apical and basolateral plasma membrane proteins in a human adenocarcinoma epithelial cell line. *Proc. Natl. Acad. Sci. USA* **86**, 9313-9317.
Lee, S. B. and Rhee, S. G. (1995). Significance of PIP_2 hydrolysis and regulation of phospholipase C isozymes. *Curr. Opin. Cell Biol.* **7**, 183-189.
Lian, L., Wang, Y., Draznin, J., Eslin, D., Bennett, J. S., Poncz, M., Wu, D. and Abrams, C. S. (2005). The relative role for PLCβ and PI3Kγ in platelet activation. *Blood* **106**, 110-117.
Lincz, L. F., Buret, A. and Burns, G. F. (1997). Formation of spheroid structures in a human colon carcinoma cell line involves a complex series of intercellular rearrangements. *Differentiation* **61**, 261-274.
Lubarsky, B. and Krasnow, M. A. (2003). Tube morphogenesis: making and shaping biological tubes. *Cell* **112**, 19-28.
Maciver, S. K. (1996). Myosin II function in non-muscle cells. *BioEssays* **18**, 179-182.
Mandato, C. A., Benink, H. A. and Bement, W. M. (2000). Microtubule-actomyosin interactions in cortical flow and cytokinesis. *Cell Motil. Cytoskeleton* **45**, 87-92.
Martin, S. G., McDonald, W. H., Yates, J. R., 3rd and Chang, F. (2005). Tea4p links microtubule plus ends with the formin for3p in the establishment of cell polarity. *Dev. Cell* **8**, 479-491.
Martin-Belmonte, F., Gassama, A., Datta, A., Yu, W., Rescher, U., Gerke, V. and Mostov, K. (2007). PTEN-mediated apical segregation of phosphoinositides controls epithelial morphogenesis through Cdc42. *Cell* **128**, 383-397.
Meberg, P. J. and Bamburg, J. R. (2000). Increase in neurite outgrowth mediated by overexpression of actin depolymerizing factor. *J. Neurosci.* **20**, 2459-2469.
Medeiros, N. A., Burnette, D. T. and Forscher, P. (2006). Myosin II functions in actin-bundle turnover in neuronal growth cones. *Nat. Cell Biol.* **8**, 215-226.
Meyer, R. D., Latz, C. and Rahimi, N. (2003). Recruitment and activation of phospholipase Cγ1 by vascular endothelial growth factor receptor-2 are required for tubulogenesis and differentiation of endothelial cells. *J. Biol. Chem.* **278**, 16347-16355.
Meyer, T. N., Schwesinger, C., Sampogna, R. V., Vaghn, D. A., Stuart, R. O., Steer, D. L., Bush, K. T. and Nigam, S. K. (2006). Rho kinase acts at separate steps in ureteric bud and metanephric mesenchyme morphogenesis during kidney development. *Differentiation* **74**, 638-647.
Millard, T. H., Sharp, S. J. and Machesky, L. M. (2004). Signalling to actin assembly via the WASP (Wiskott-Aldrich syndrome protein)-family proteins and the Arp2/3 complex. *Biochem. J.* **380**, 1-17.
Minamide, L. S., Shaw, A. E., Sarmiere, P. D., Wiggan, O., Maloney, M. T., Bernstein, B. W., Sneider, J. M., Gonzalez, J. A. and Bamburg, J. R. (2003). Production and use of replication-deficient adenovirus for transgene expression in neurons. *Methods Cell Biol.* **71**, 387-416.
Moore, K. A., Polte, T., Huang, S., Shi, B., Alsberg, E., Sunday, M. E. and Ingber, D. E. (2005). Control of basement membrane remodeling and epithelial branching morphogenesis in embryonic lung by Rho and cytoskeletal tension. *Dev. Dyn.* **232**, 268-281.
Morton, W. M., Ayscough, K. R. and McLaughlin, P. J. (2000). Latrunculin alters the actin-monomer subunit interface to prevent polymerization. *Nat. Cell Biol.* **2**, 376-378.
Motegi, A., Fujimoto, J., Kotani, M., Sakuraba, H. and Yamamoto, T. (2004). ALK receptor tyrosine kinase promotes cell growth and neurite outgrowth. *J. Cell Sci.* **117**, 3319-3329.
Mouneimne, G., Soon, L., DesMarais, V., Sidani, M., Song, X., Yip, S. C., Ghosh, M., Eddy, R., Backer, J. M. and Condeelis, J. (2004). Phospholipase C and cofilin are required for carcinoma cell directionality in response to EGF stimulation. *J. Cell Biol.* **166**, 697-708.
Mouneimne, G., DesMarais, V., Sidani, M., Scemes, E., Wang, W., Song, X., Eddy, R. and Condeelis, J. (2006). Spatial and temporal control of cofilin activity is required for directional sensing during chemotaxis. *Curr. Biol.* **16**, 2193-2205.
Nobes, C. D. and Hall, A. (1995). Rho, rac and cdc42 GTPases: regulators of actin structures, cell adhesion and motility. *Biochem. Soc. Trans.* **23**, 456-459.
O'Brien, L. E., Jou, T. S., Pollack, A. L., Zhang, Q., Hansen, S. H., Yurchenco, P. and Mostov, K. E. (2001). Rac1 orientates epithelial apical polarity through effects on basolateral laminin assembly. *Nat. Cell Biol.* **3**, 831-838.
O'Brien, L. E., Zegers, M. M. and Mostov, K. E. (2002). Opinion: building epithelial architecture: insights from three-dimensional culture models. *Nat. Rev. Mol. Cell Biol.* **3**, 531-537.
O'Connell, C. B., Tyska, M. J. and Mooseker, M. S. (2007). Myosin at work: motor adaptations for a variety of cellular functions. *Biochim. Biophys. Acta* **1773**, 615-630.
Olson, A. D., Pysher, T. and Bienkowski, R. S. (1991). Organization of intestinal epithelial cells into multicellular structures requires laminin and functional actin microfilaments. *Exp. Cell Res.* **192**, 543-549.
Ono, S. (2007). Mechanism of depolymerization and severing of actin filaments and its significance in cytoskeletal dynamics. *Int. Rev. Cytol*. **258**, 1-82.
Pelish, H. E., Peterson, J. R., Salvarezza, S. B., Rodriguez-Boulan, E., Chen, J. L., Stamnes, M., Macia, E., Feng, Y., Shair, M. D. and Kirchhausen, T. (2006). Secramine inhibits Cdc42-dependent functions in cells and Cdc42 activation in vitro. *Nat. Chem. Biol.* **2**, 39-46.
Powis, G., Seewald, M. J., Gratas, C., Melder, D., Riebow, J. and Modest, E. J. (1992). Selective inhibition of phosphatidylinositol phospholipase C by cytotoxic ether lipid analogues. *Cancer Res.* **52**, 2835-2840.
Ramoni, C., Spadaro, F., Menegon, M. and Podo, F. (2001). Cellular localization and functional role of phosphatidylcholine-specific phospholipase C in NK cells. *J. Immunol.* **167**, 2642-2650.
Rhee, S., Jiang, H., Ho, C. H. and Grinnell, F. (2007). Microtubule function in fibroblast spreading is modulated according to the tension state of cell-matrix interactions. *Proc. Natl. Acad. Sci. USA* **104**, 5425-5430.
Rogers, K. K., Jou, T.-S. and Lipschutz, J. H. (2003). The Rho family of small GTPases is involved in epithelial cystogenesis and tubulogenesis. *Kidney Int.* **63**, 1632-1644.
Rosenblatt, J., Cramer, L. P., Baum, B. and McGee, K. M. (2004). Myosin II-dependent cortical movement is required for centrosome separation and positioning during mitotic spindle assembly. *Cell* **117**, 361-372.
Sarmiere, P. D. and Bamburg, J. R. (2004). Regulation of the neuronal actin cytoskeleton by ADF/cofilin. *J. Neurobiol.* **58**, 103-117.
Scaife, R. M., Job, D. and Langdon, W. Y. (2003). Rapid microtubule-dependent induction of neurite-like extensions in NIH 3T3 fibroblasts by inhibition of ROCK and Cbl. *Mol. Biol. Cell* **14**, 4605-4617.
Schmeichel, K. L. and Bissell, M. J. (2003). Modeling tissue-specific signaling and organ function in three dimensions. *J. Cell Sci.* **116**, 2377-2388.
Schock, F. and Perrimon, N. (2002). Molecular mechanisms of epithelial morphogenesis. *Annu. Rev. Cell Dev. Biol.* **18**, 463-493.
Scott, E. K. and Luo, L. (2001). How do dendrites take their shape? *Nat. Neurosci.* **4**, 359-365.
Straight, A. F., Cheung, A., Limouze, J., Chen, I., Westwood, N. J., Sellers, J. R. and Mitchison, T. J. (2003). Dissecting temporal and spatial control of cytokinesis with a myosin II Inhibitor. *Science* **299**, 1743-1747.
Suurna, M. V., Ashworth, S. L., Hosford, M., Sandoval, R. M., Wean, S. F., Shah, B. M., Bamburg, J. R. and Molitoris, B. A. (2006). Cofilin mediates ATP depletion-induced endothelial cell actin alterations. *Am. J. Physiol. Renal Physiol.* **290**, F1398-F1407.
Takenawa, T. and Suetsugu, S. (2007). The WASP-WAVE protein network: connecting the membrane to the cytoskeleton. *Nat. Rev. Mol. Cell Biol.* **8**, 37-48.
Tornieri, K., Welshhans, K., Geddis, M. S. and Rehder, V. (2006). Control of neurite outgrowth and growth cone motility by phosphatidylinositol-3-kinase. *Cell Motil. Cytoskeleton* **63**, 173-192.
Walpita, D. and Hay, E. (2002). Studying actin-dependent processes in tissue culture. *Nat. Rev. Mol. Cell Biol.* **3**, 137-141.

Wang, W., Eddy, R. and Condeelis, J. (2007). The cofilin pathway in breast cancer invasion and metastasis. *Nat. Rev. Cancer* **7**, 429-440.

Waterman-Storer, C. M., Worthylake, R. A., Liu, B. P., Burridge, K. and Salmon, E. D. (1999). Microtubule growth activates Rac1 to promote lamellipodial protrusion in fibroblasts. *Nat. Cell Biol.* **1**, 45-50.

Xie, Y., Hong, Y., Ma, X. Y., Ren, X. R., Ackerman, S., Mei, L. and Xiong, W. C. (2006). DCC-dependent phospholipase C signaling in netrin-1-induced neurite elongation. *J. Biol. Chem.* **281**, 2605-2611.

Xu, B., Pelish, H., Kirchhausen, T. and Hammond, G. B. (2006). Large scale synthesis of the Cdc42 inhibitor secramine A and its inhibition of cell spreading. *Org. Biomol. Chem.* **4**, 4149-4157.

Yin, H. L. and Janmey, P. A. (2003). Phosphoinositide regulation of the actin cytoskeleton. *Annu. Rev. Physiol.* **65**, 761-789.

Yvon, A. M., Gross, D. J. and Wadsworth, P. (2001). Antagonistic forces generated by myosin II and cytoplasmic dynein regulate microtubule turnover, movement, and organization in interphase cells. *Proc. Natl. Acad. Sci. USA* **98**, 8656-8661.

Zhang, J., Betson, M., Erasmus, J., Zeikos, K., Bailly, M., Cramer, L. P. and Braga, V. M. (2005). Actin at cell-cell junctions is composed of two dynamic and functional populations. *J. Cell Sci.* **118**, 5549-5562.

Zhou, F. Q., Waterman-Storer, C. M. and Cohan, C. S. (2002). Focal loss of actin bundles causes microtubule redistribution and growth cone turning. *J. Cell Biol.* **157**, 839-849.